

Lamellar Double Hydroxides Intercalated with Humic Substances and Nitrate: Evaluation of Phosphate Removal in Water and Application in Agricultural Sectors

Amanda P. B. da Silva,^a Oseas S. Santos,^b Luciana C. de Oliveira,^c Sivaldo Paulino^a and Wander G. Botero^{ib}*,^a

^aPrograma de Pós-Graduação em Química e Biotecnologia, Universidade Federal de Alagas (UFAL), 57309-005 Maceió-AL, Brazil

^bUniversidade Estadual do Mato Grosso do Sul (UEMS), 79730-000 Glória de Dourados-MS, Brazil

^cPrograma de Pós-Graduação em Biotecnologia e Monitoramento Ambiental, Departamento de Física, Química e Matemática, Universidade Federal de São Carlos (UFSCar), 13506-900 Sorocaba-SP, Brazil

Phosphate species can affect aquatic ecosystems, as excess of this nutrient can cause eutrophication, generating environmental impacts. Lamellar double hydroxides have shown promise in removing phosphate at low concentrations (10-50 mg L⁻¹). In this context, lamellar double hydroxides were synthesized interspersed with nitrates and humic substances, searching for a new product that favors phosphorus adsorption. X-ray diffraction showed the presence of characteristic peaks of lamellar double hydroxides and thermogravimetric analysis showed the decomposition behavior of lamellar structure. The adsorption capacity occurred quickly (< 30 min), being more efficient for lamellar double hydroxides with NO₃. The maximum adsorption capacity showed results of 35.03 and 44.20 mg g⁻¹ for lamellar double hydroxides with humic substances and lamellar double hydroxides with NO₃, respectively. The complexation capacity showed that pH directly influences complexation, being greater for lamellar double hydroxides with humic substances at pH 6.5. Thus, nanostructured materials with humic substances are promising for use in contaminant remediation and adsorption can be a fast and efficient technique for use in soil and water.

Keywords: lamellar double hydroxides, humic substances, adsorption, phosphate

Introduction

In 2022, the world population reached 8 billion inhabitants and it is estimated that by 2037 this number will reach 9 billion.¹ As a consequence of this growth, there is an increase in environmental problems and significant challenges related to the increase in food demand of the population of the world. In seeking to meet this great demand for food, the excessive dependence on chemical fertilizers harms both the environmental ecology and human health. The indiscriminate use of chemical fertilizers poses a great threat to nature by polluting the air, water, and soil.^{2,3}

Among the nutrients applied to the soil, the low availability of phosphorus is a reality in most Brazilian soils. It is estimated that 5.7 billion hectares of soil

worldwide are deficient in this element.⁴ Therefore, phosphate fertilization is necessary to increase P levels in the soil, since this nutrient plays a fundamental role in the metabolism process of plants, as it performs the function of storing and transferring energy in the cell, in respiration and photosynthesis, a fundamental process related to productivity. On the other hand, there is a long-term concern, since high-quality phosphate ore reserves are limited.^{5,6}

An alternative to this problem has been the use of organic fertilizers, as they provide improvements in the physical, chemical, and biological attributes of the soil, contributing to plant growth.^{7,8} However, organic fertilizers, such as manure and/or compost, commonly used in organic systems, have low concentrations of nutrients, including phosphorus, a fact that implies the use of high volumes, increasing costs with transport and application in addition to the decrease in productivity.⁹

*e-mail: wander.botero@iqb.ufal.br

Editor handled this article: Maria Cristina Canela (Associate)



In addition to its action as a macronutrient in agriculture, once in the environment in significant concentrations, it can become a polluting agent in natural waters, acting in the proliferation of algae, eutrophication, reduction of dissolved oxygen in these waters and production of toxins.

In this context, the search for adsorption methods for removing phosphate in water has been the subject of study by different researchers.¹⁰⁻¹⁴ Phosphate adsorption removal is particularly attractive and the possibility of associated recovery and subsequent reuse of the removed phosphate in agricultural environments makes it even more interesting from an environmental, social, and economic point of view.

An alternative as a support for the contaminants adsorption has been lamellar double hydroxides (LDH), which are part of the class of nanostructured anionic clay compounds. LDH structures consist of brucite-type lamellas ($\text{Mg}(\text{OH})_2$) where magnesium cations are located inside the octahedra and with hydroxyl anions at their apexes, remaining stacked through hydrogen bonds. To stabilize these lamellae, hydrated anions, which can be inorganic or organic, are interspersed, promoting a stacking of the hydroxide layers. Thus, in addition to hydrogen bonds, these lamellae also remain connected by electrostatic attractions between the positively charged lamellae and the interlamellar anions.¹⁵

Most LDH are easily synthesized using low-cost materials and unsophisticated equipment. Studies^{16,17} show that this adsorbent has a high capacity to remove phosphorus from effluents in which the element concentration is low.

One of the main advantages of using LDH in agriculture is the possibility of regenerating the material at the end of the process, in addition to being able to recover the phosphorus itself and use it as a nutrient in biological cycles.^{18,19}

In addition to LDH, humic substances (HS) are of great environmental, technological, and agricultural interest, as they have high levels of carboxyl groups, phenolic hydroxyls, alkyl and nitrogenous groups, which provide interaction with nutrients and contaminants, influencing their availability in the environment.²⁰⁻²³

Thus, integrating two types of effective adsorption components such as LDH and humic substances can present a new material with improved performance or with new properties, since this material can retain its anion exchange capacity after loading the HS, providing the adsorption capacity for both anion exchange and complexation of potentially toxic metals.

The development of LDH-based materials with high selectivity towards phosphate can achieve high removal efficiencies and contribute to the possibility of recovering and reusing the removed phosphate.

Thus, this work synthesized and characterized lamellar double hydroxides interspersed with nitrates and humic substances, seeking a new product with characteristics that favor the adsorption of phosphate for environmental remediation and subsequent application in agriculture, providing nutrients (N and P) and organic matter originating from the humic substances.

Experimental

Reagents and solutions

All reagents used were analytical grade and purchased from Merck (Darmstadt, Germany) and Sigma-Aldrich (St. Louis, USA). All solutions were prepared with ultrapure water obtained from the Gehaka system (São Paulo, Brazil) with $18.2 \text{ M}\Omega \text{ cm}$ (at $25 \text{ }^\circ\text{C}$). Before use, all working materials were previously washed with 10% (v/v) HNO_3 and ultrapure water. For nutrient and contaminant studies, standard solutions of the chemical elements were prepared by diluting commercial stock solutions of 1000 mg L^{-1} (Merck, São Paulo, Brazil).

Synthesis of LDH and LDH with humic substances

For LDH-HS synthesis, humic substances extracted from peat samples were used. The synthesis of LDH-HS was carried out by the coprecipitation method at pH 10, according to the methodology adopted by Reichle.²⁴ It was prepared in a molar ratio (5:1) from mixed metallic solutions containing magnesium nitrate hexahydrate ($\text{Mg}(\text{NO}_3)_2 \cdot 6\text{H}_2\text{O}$) and aluminum nitrate nonahydrate ($\text{Al}(\text{NO}_3)_3 \cdot 9\text{H}_2\text{O}$) dissolved in deionized water.

The metal solution was slowly dripped into the solution of humic substances (100 mg L^{-1}) and simultaneously a slow addition of a 1 mol L^{-1} sodium hydroxide (NaOH) solution was also performed, used to maintain a constant pH of approximately 10. The procedure was carried out under mechanical agitation and at room temperature. After the addition of the entire metallic solution, the LDH was aged for 2 h. The compound formed was centrifuged for 10 min to separate the phases and then washed 5 times with deionized water to remove excess humic substances. The resulting gel was left in an oven at $60 \text{ }^\circ\text{C}$ for 24 h and the material obtained was macerated with a pestle until obtaining a powder.

For LDH- NO_3 synthesis, the same procedure was adopted, using an 80 mg L^{-1} sodium nitrate solution (NaNO_3), which contained enough NO_3^- for the molar ratio with M^{3+} to be four times greater than that necessary for the intercalation of NO_3^- ions, which is proportional to the content of Al^{3+} ions in the structure.

Materials characterization

X-ray diffraction and thermogravimetric analysis

X-ray diffraction (XRD) patterns were collected using a Shimadzu LabX XRD-6000 (Kyoto, Japan) diffractometer with a graphite monochromator, operating at 40 kV and 30 mA and Cu K α radiation ($\lambda = 0.1542$ nm), operating in the range from 1.4 to 80° (2 θ) and sweep speed at 2° min⁻¹. These analyses aimed to identify and determine the crystalline phases, as well as the structural properties of the materials.

For the thermogravimetric analysis (TGA), 10 mg of the LDH sample were subjected to a temperature range of 30 to 900 °C, with a heating rate of 10 °C min⁻¹, in an inert atmosphere (N₂), using a DTG-60TG (Shimadzu, Kyoto, Japan), simulating pyrolysis conditions.²⁵

Phosphate ion adsorption by LDH intercalated with humic substances and nitrate

Adsorption experiments were carried out to investigate the adsorption kinetics of phosphate ions on LDH-HS and LDH-NO₃. A mass of 0.1 g of the synthesized material was added to four 100 mL KH₂PO₄ solutions with concentrations of 15, 20, 25, and 50 mg L⁻¹, respectively. The suspensions were stirred at room temperature. The pH was maintained at 8.0 using 0.1 mol L⁻¹ NaOH to ensure good preservation of the LDH structure. A 5 mL aliquot of the suspension was withdrawn at time intervals of 30, 60, 120, 180, 240, 360, 720, and 1440 min.

Complexing capacity of LDH intercalated with humic substances and nitrate by phosphate

To determine the complexing capacity of LDH intercalated with HS and phosphate nitrate, 250 mL of a 100 mg L⁻¹ solution of LDH-HS and LDH-NO₃ were subjected to a tangential ultrafiltration system equipped with a 1-mm cellulose membrane kDa (Millipore, Billerica, USA) at pH 6.5 and 8.0. This system evaluates the speciation of phosphate ions, separating free phosphate from complexed phosphate, LDH-HS, and LDH-NO₃. After conditioning the membrane for 5 min, the first aliquot called T₀ (about 2 mL) was filtered, corresponding to time zero (without adding the mercury solution). Subsequent aliquots were obtained by adding 0.02; 0.02; 0.02; 0.02; 0.02; 0.1; 0.2; 0.6; 1 and 2 mL of a 500 mg L⁻¹ phosphate(II) solution being filtered after 30 min of contact between each addition.

Determination of phosphate ions

Phosphate quantification was performed using the

vanadate yellow colorimetric method.²⁶ The method consists of a mixed reagent containing two solutions. Solution A: 5% ammonium molybdate (NH₄)₆Mo₂O₂₄·4H₂O and solution B: 0.25% ammonium metavanadate (NH₄VO₃). A 50/50 mixture of the two solutions was made and then 2 mL of the sample was placed in contact with 0.5 mL of the mixed solution, stirred, and after 15 min, reading was taken on a UV-Vis spectrophotometer (mono-beam) UV-M51-Bel (Piracicaba, Brazil) at 420 nm. Analyses were performed in duplicate. The reaction of this with molybdate in an acid medium produces a mixed molybdate/phosphate complex which, in the presence of the vanadate ion, forms molybdovanadophosphoric acid, which is yellowish. The intensity of the yellow color is proportional to the concentration of phosphate ions in the sample.

Results and Discussion

X-ray diffraction (XRD)

On lamellar hydroxides synthesis, X-ray diffraction is of great importance, as it is from this analysis that the formation of the lamellar material is identified. To confirm the lamellar structures, the samples were characterized by XRD.

Hydrotalcite-type materials were obtained, evidenced by the presence of well-defined and characteristic diffraction peaks such as planes 110 and 113 (Figure 1).²⁷

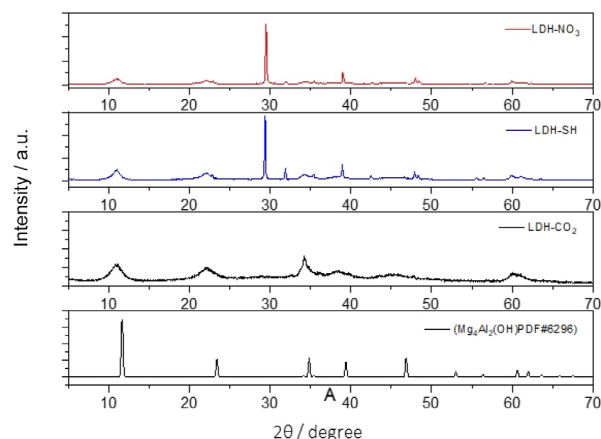


Figure 1. X-ray powder diffraction for LDH-NO₃, LDH-HS and LDH-CO₂ samples. (Mg₃Al₂(OH)₆)₂(OH)₂CO₃ PDF #6296) inorganic crystal structure database.

Interlamellar distances were calculated using the Bragg equation:

$$n\lambda = 2d_{hkl} \quad (1)$$

where: $n\lambda$ is the diffraction order (normally $n = 1$); λ is the wavelength of incident radiation; d_{hkl} is the interplanar distance.

The values obtained (Table 1) indicate that the partial or total replacement of magnesium ions affected the basal spacing in the hydrotalcite structure.²⁸

From the lines (003) and (006) positions, the basal hydrotalcite spacings were calculated and used to determine the lattice parameter *c*, which corresponds to 3 times the distance between adjacent hydroxide layers.

The decrease in parameter *c* (basal spacing) is related to the Al³⁺ content in the samples. The higher content of Al³⁺ ions in the lamellae increases the attractive Coulomb forces between the positively charged layers and the CO₃²⁻ anions, decreasing the basal spacing. The increase in the parameter *a* is also related to the Al³⁺ content in the samples. With a decrease in Al³⁺ content, which has an ionic radius smaller than Mg²⁺ (*r*Mg = 0.72 and *r*Al = 0.53), there is an increase in the value of parameter *a*.

From the results obtained in the Table 1, it is possible

to observe a small increase in the basal spacing, which indicates intercalation of fulvic and humic acid groups between the LDH layers. According to Li *et al.*,²⁹ HS fractions can be effectively and stably anchored on the surface of LDH through the coagulation process, occupying the intermediate layer of LDH.

Intercalation of whole HS molecules into the intermediate layer of LDH is unlikely to occur. Probably, only small parts of the molecules can be intercalated between the brucite-like sheets, which can be confirmed by the small increase in the *d*003 spacing of these LDH after intercalation of the humic substances.

The decrease in basal distances occurs due to the decrease in the average ionic radius of the precursor metals that make up these materials.³⁰

The thermogram for the synthesized materials is presented in Figure 2. The thermal behavior of the materials

Table 1. Interlayer and edge spacing results calculated for the LDH-HS, LDH-NO₃ and LDH-CO₃ samples

Plan	LDH-HS				LDH-NO ₃				LDH-CO ₃			
	Peak (2θ) / degree	d / Å	a / nm	c / Å	Peak (2θ) / degree	d / Å	a / nm	c / Å	Peak (2θ) / degree	d / Å	a / nm	c / Å
(003)	10.94	8.09	2.42	24.27	11.01	8.03	1.39	24.09	10.88	8.13	1.41	24.39
(006)	22.14	4.01	0.80	12.03	22.87	3.88	0.77	11.64	22.11	4.02	0.80	12.06
(009)	29.36	3.04	1.05	9.12	29.42	3.03	0.85	9.09	34.20	2.62	0.74	7.86
(101)	31.86	2.81	1.22	8.43	31.94	2.80	1.22	8.40	38.62	2.33	1.01	6.99
(012)	35.38	2.53	0.87	7.59	35.46	2.53	0.87	7.59	45.19	2.00	0.69	6.00
(015)	38.94	2.31	0.92	6.93	39.01	2.30	0.92	6.90	61.10	1.51	0.60	4.53
(107)	42.48	2.12	0.92	6.36	42.65	2.12	0.92	6.36	–	–	–	–
(018)	47.90	1.89	0.84	5.67	48.46	1.87	0.83	5.61	–	–	–	–

LDH: lamellar double hydroxides; HS: humic substances; d: interplanar distance; a: edges; c: basal spacing ($c = 3 \times d(003)$).

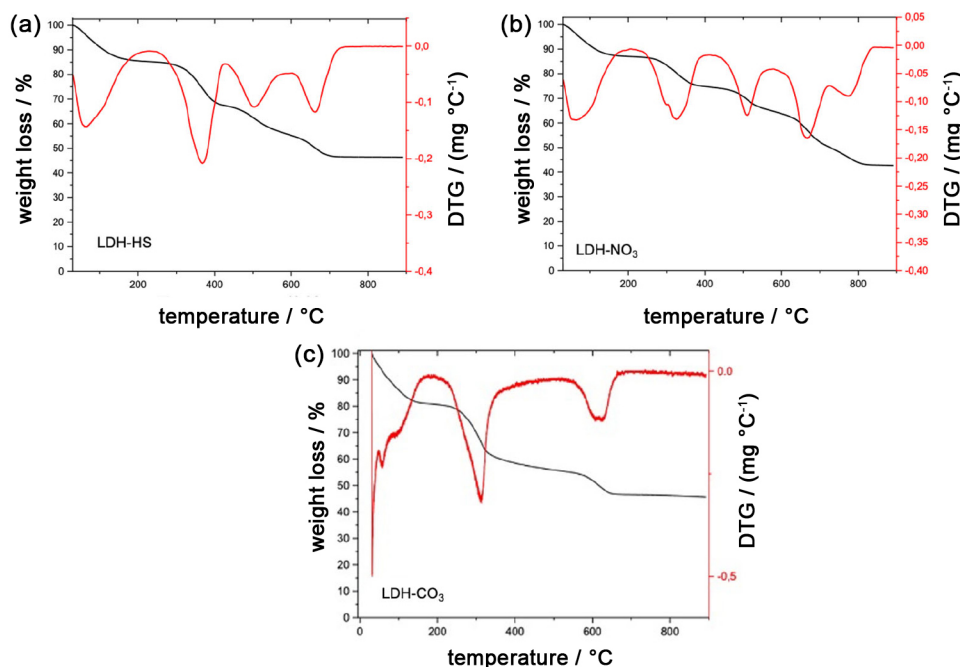


Figure 2. Characterization of TGA/differential thermogravimetric analysis (DTG) as a function of temperature: (a) LDH-HS, (b) LDH-NO₃ and (c) LDH-CO₃.

corroborates the literature with important loss events. The first stage of weight loss occurs in the temperature range of 30-210 °C, with weight loss of 14.4, 12.9 and 19.2% of LDH-HS, LDH-NO₃ and LDH-CO₃ respectively, which is associated with water removal from the intermediate layer and adsorbed water molecules without collapse of the structure. In the second stage, in the range of 210-420 °C, the thermal decomposition of hydrotalcite and weight loss were 17.3, 12.4 and 24.1%, which can be attributed to the decomposition of hydroxyl groups in the layers and intercalated carbonates and nitrates.³¹

The third stage of decomposition occurs from 420-590 °C. At this stage, the weight loss was 12.5, 10.3 and 8.7%, which is possibly related to the dehydroxylation of OH linked to the aluminum cation present inside the lamella, OH limited by a magnesium cation and the main decarbonization by CO₂.³²

Finally, the fourth stage occurred between 590 and 720 °C with a loss of 9.3 and 13.7% in mass content resulting from the decomposition of the other hydroxyl groups,³¹ which varies according to the chemical nature of the sample.

It is important to highlight that for LDH-HS and LDH-NO₃ there were four loss events, while for LDH-CO₃ only three loss events. This may be related to the decomposition of insoluble impurities, which could not be removed during the washing process of the synthesized materials.³²

XRD data from LDH samples showed lamellar structures and basal reflection planes of LDH with interlayer spacing of 8.09, 8.03 and 8.13 Å for LDH-HS, LDH-NO₃ and LDH-CO₃, respectively. The TGA thermogram of LDH showed the decomposition behavior of the lamellar structure, confirming that the synthesized products are lamellar double hydroxides.

Phosphate adsorption studies

Adsorption is among the best alternatives for removing organic pollutants, pharmaceuticals, and other

contaminants.³³ LDHs are used to remove various types of ions in aqueous solutions by adsorption, as they have characteristics that favor this process, such as good thermal and chemical stability.^{34,35}

The contact time indicates the kinetic behavior of adsorption for a given adsorbent at a given initial adsorbate concentration. The effect of contact time for phosphate ions adsorption on LDH-HS and LDH-NO₃ subjected to different phosphate concentrations indicated maximum adsorption of around 30 min of contact (Figure 3).

Phosphate ions are variable during the initial times of adsorption. According to Yu *et al.*³⁶ this is due to the amount of active sites available for sorption on the surface. However, with increasing surface coverage, the number of remaining binding sites decreases, resulting in a decrease in the repulsive forces between adsorbed and free molecules, leading to the equilibrium state.

All analyzed concentrations present fast adsorption, it is noted that the amount adsorbed remains variable in the first 300 min (LDH-HS) and remains constant after that time. For LDH-NO₃, the adsorption behavior was similar for all analyzed concentrations. The equilibrium time was approximately the same regardless of concentrations and material (Figure 3) corroborating other studies in the literature³⁷⁻³⁹ with materials used in adsorption studies.

At the concentration of 50 mg L⁻¹, the percentage of adsorption was ca. 70%, which corresponds to 35.00 mg g⁻¹ for LDH-HS, while for LDH-NO₃ at the same concentration, it was ca. 88%, equivalent to 44.00 mg g⁻¹. Huang *et al.*,³⁹ in their study using hydrotalcite (Mg-Al-CO₃) to remove phosphate in drinking water, obtained a percentage of 19.6% which corresponds to 9.68 mg when using a concentration of 50 mg L⁻¹ of phosphorus, thus showing that materials synthesized with humic substances and nitrate present promising results.

In general, when we compare the percentage of adsorption for the two samples (LDH-HS and LDH-NO₃), it can be seen that the adsorption of LDH-NO₃ is more

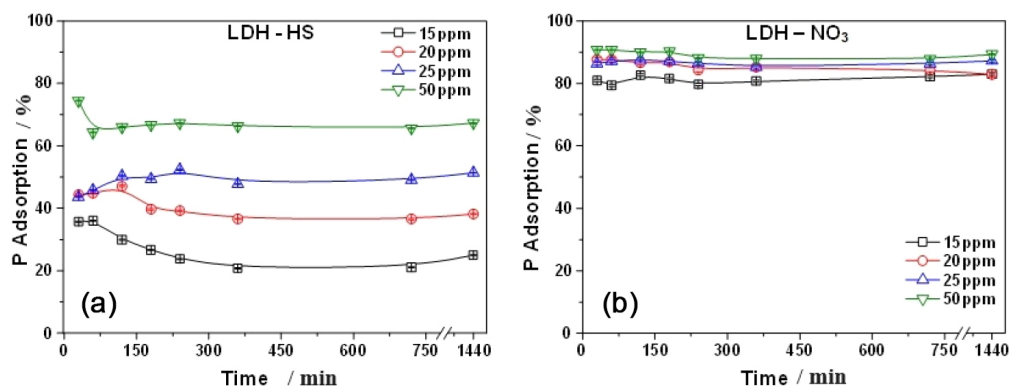


Figure 3. Effect of contact time on different concentrations of phosphate ions: (a) LDH-HS and (b) LDH-NO₃.

efficient than that of LDH-HS, which can be attributed to the structure of the material produced and the intercalated anion since humic substances have larger structures.

Studies proposed by Li *et al.*²⁹ indicate that the structure and size of the anion play an important role in the specific interaction between LDH and intercalated anion.

Although LDH-NO₃ presents a higher percentage of adsorption, the adsorption variation is low (ca. 10%) when we analyze the concentration variation (15 to 50 mg L⁻¹), showing that the concentration is not a determining factor for this type of material. As for LDH-HS, this percentage difference (ca. 40%) is more evident, with better adsorption to the analyzed concentrations.

Another important factor to be highlighted is the influence of pH on these materials adsorption, since both experiments were carried out at the same pH 7, it is noted that for LDH-HS the percentage of adsorption was lower. According to Borges,⁴⁰ the efficiency in the adsorption of humic substances is greater in an acid medium (pH < 7.0) due to the hydrophobic bonds that occurred between the surface of the sand and clay with the adsorbate.

According to Borges,⁴⁰ at lower pH humic acid molecules are more contracted because the carboxylic groups are more protonated causing a lower intramolecular electrostatic repulsion. With this, there is greater adsorption due to an increase in the ease of humic acid molecules to penetrate the pores of the adsorbent.

The tests performed by Petzold *et al.*⁴¹ aimed to evaluate the influence of humic acid adsorption on clay in the flocculation of these clays. Through analysis of the adsorption isotherm of humic acid on clay at 20 °C and pH between 7 and 8, the anionic characteristics of clay suspensions were observed. They observed an increase in negative charges on clay after humic acid adsorption and also that only 40% of humic acid was adsorbed under these conditions.

The adsorption of humic acid on clay was also reported

by Liu and Gonzalez.⁴² According to the researchers, with pH increase, there was a 50% decrease in the adsorption of humic acid. This fact was explained by the increase in repulsion between the negative charges on the clay surface and the negative charges on the humic acid molecules present in the HS.

Comparing the results obtained with those in the literature (Table 2), it is possible to observe that the maximum adsorption capacity of the synthesized materials presented better results.

LDH have a good ion exchange capacity, which works by replacing the guest anion between the layers with the target anion, such as phosphate species.⁴³ In this sense, LDH-HS has an advantage in its application, since these exchanges of humic fractions for phosphate species can benefit the soil.

For LDH-NO₃, the adsorption capacity showed better results that may be related to the type of interlayer anion, since the interlayer anion and the charge density are responsible for the anion exchange capacity of an LDH. The higher charge density value is unfavorable because the displacement of the interlayer anion with the target anion becomes more difficult.⁴⁴ Therefore, Mg-type LDH having NO₃⁻ as interlayer anions are good anion exchangers because of the weak interlayer electrostatic interaction. An advantage of anion exchange is that pH adjustment is not required, and LDH can function over a wide pH range without being damaged.⁴⁵

The fact that phosphate is a non-renewable resource encourages researchers to find ways to recover it. Meanwhile, the accumulation of phosphate in water sources because of agricultural activities or wastewater discharges causes serious environmental problems such as eutrophication. Therefore, phosphate recovery is of great importance, it not only avoids environmental pollution but also results in a raw material with economic value.

In this sense, in recent decades, LDH have attracted considerable attention as ecological materials due also to

Table 2. Adsorption capacity of some adsorbents reported in the literature compared to this work

Material	Mass / mg	Adsorbate	Maximum adsorption capacity / (mg g ⁻¹)	Reference
LDH-CO ₃	100	phosphate	23.79	46
LDH-biochar	800	arsenic	10.4	47
Biochar	800	arsenic	0.42	47
Hydrochar modified MgAl-LDHs derived from tobacco stem	100	phosphate	30.69	48
Humins	100	phosphate	11.53	49
LDH-HS	100	phosphate	35.03	this work
LDH-NO ₃	100	phosphate	44.2	this work

LDH: lamellar double hydroxides; HS: humic substances.

their excellent ability to remove various harmful anions,^{39,44} heavy metals⁴⁴ and organic pollutants.⁵⁰⁻⁵²

Complexing capacity of LDH intercalated with humic substances and nitrate by phosphate

Several techniques have been used to determine the complexing capacity, such as voltammetry, potentiometry, ultrafiltration, and chromatography. The advantage of ultrafiltration over other analytical strategies is associated with its versatility, being able to be used in different adsorbents or adsorbed material, where the separation method is a physical process, allowing its use in different pH and ionic strengths.⁵³⁻⁵⁵

The complexing capacity (CC) is generally expressed by the amount of analyte that saturates the sites of interaction with the materials (LDH-HS and LDH-NO₃). CC is influenced by factors such as adsorbent concentration, concentration of species to be complexed (adsorbed), pH, temperature, ionic strengths, and other aspects.⁵⁶⁻⁵⁸

The complexing ability of LDH-HS and LDH-NO₃ by phosphate (Figure 4) was determined by the intersection of the two curves related to the concentration of free (not binding to LDH) and total phosphate.⁵⁶ The pH is one of the most important factors in the complexing capacity, as it is related to the protonation of the functional groups of humic substances, favoring or not the complexation²⁰ of chemical species. The complexing capacity values for LDH-HS are 23.32 mg g⁻¹ at pH 6.5 and 13.21 mg g⁻¹ at pH 8.0 and for LDH-NO₃ it is 19.11 mg g⁻¹ at pH 6.5 and 21.52 mg g⁻¹ at pH 8.0.

Oliveira *et al.*⁴⁹ determined the CC content for humin with phosphate ions and obtained values of 11.53 mg g⁻¹ of humin. When comparing the results obtained, it is observed that LDH-HS had a greater complexing capacity with phosphate ions than LDH-NO₃ at pH 6.5. This increase may be associated with functional groups increase, derived from HS, in LDH, contributing to a greater interaction and corroborating with the adsorption data. Botero *et al.*⁵⁶ determined the CC for samples of humic substances from

peat obtaining values of 8.73 mg g⁻¹ for Cu^{II}. Souza *et al.*⁵⁹ determined CC for humic substances from soils and water with CN⁻ ions and obtained values between 3.69 and 7.2 mg g⁻¹, respectively.

However, at pH 8.0, there is a decrease in the complexing capacity for LDH-HS and phosphate ions and an increase for LDH-NO₃, corroborating the adsorption data and which may be associated with a greater repulsion of the HS functional groups in the LDH-HS, thus decreasing its complexing capacity. In this sense, in general, the highest complexations occurred with LDH-HS at pH 6.5, which suggests a high interaction between this material and phosphate ions.

Conclusions

This work proposes the use of LDH as adsorbents in order to investigate the adsorption kinetics of phosphate ions. According to the results presented in the present work, it is concluded that the synthesis of LDHs containing humic substances, nitrate and carbonate using the coprecipitation method was satisfactory. For the XRD analysis of the materials, the graph presents well-defined diffraction peaks (planes 110 and 113) and characteristic of the hydrotalcite-like structure.

In recent years there has been a considerable increase in cases of pollution of water resources, such as eutrophication caused by excessive concentration of phosphate. With the potential use of LDH as adsorbents to remove these species, studies report that this adsorption capacity generally occurs for a synthetic solution containing high initial concentrations of phosphate.

However, the present work was carried out at different concentrations (ranging from 15 to 50 mg L⁻¹), and the kinetic studies with phosphate showed good adsorption results with ca. 70% for LDH-HS and for LDH-NO₃ ca. 88% of phosphate ions, where the lowest percentage rate may be related to the pH of the study, since humic substances have better adsorption efficiency at acidic pH. It is also possible to observe that after 300 min the adsorption

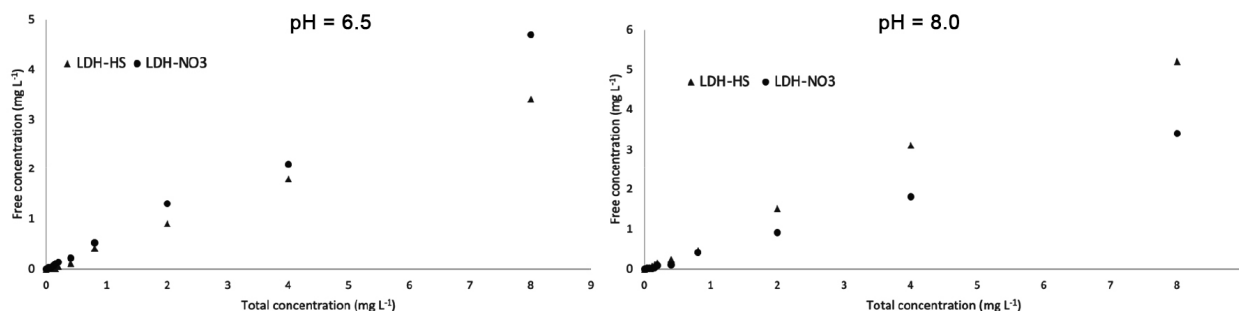


Figure 4. Complexation capacity curve for LDH-HS and LDH-NO₃ with phosphate ions using the tangential ultrafiltration technique at pH 6.5 and 8.0.

rate remains constant for both materials.

The complexing capacity showed high interaction with phosphate ions being for LDH-HS: 23.32 mg g⁻¹ at pH 6.5 and 13.21 mg g⁻¹ at pH 8.0 and for LDH-NO₃: 19.11 mg g⁻¹ at pH 6.5 and 21.52 mg g⁻¹ at pH 8.0.

Regarding the intercalation of humic substances in the LDH, from the results obtained it was possible to observe a small increase in the basal spacing that indicates an intercalation of groups of fulvic and humic acids between the layers of the LDH

In this sense, the use of LDH for phosphate ions removal is feasible, and can be used in the effluents treatment, due to the low cost and the high adsorption capacity in such a short time and demonstrate the potential use of LDH with possibilities of applications as well in agricultural systems.

Author Contributions

Amanda P. B. da Silva was responsible for data curation, formal analysis, investigation, methodology, validation, visualization and writing (original draft, review and editing); Oseas S. Santos for data curation, formal analysis, methodology, software and writing original draft; Luciana C. de Oliveira for conceptualization, data curation, methodology, resources, software, supervision and writing (original draft, review and editing); Sivaldo Paulino for data curation, investigation, methodology, supervision and writing (original draft, review and editing); Wander G. Botero for conceptualization, data curation, funding acquisition, project administration, supervision, validation, visualization and writing (original draft, review and editing).

References

1. Nações Unidas, *NU News*, <https://brasil.un.org/pt-br/189756-popula%C3%A7%C3%A3o-mundial-chegar%C3%A1-8-bilh%C3%B5es-em-novembro-de-2022>, accessed in June 2024.
2. Savci, S.; *Int. J. Environ. Sci. Dev.* **2012**, *3*, 73. [Crossref]
3. Jariwala, H.; Santos, R. M.; Lauzon, J. D.; Dutta, A.; Chiang, Y. W.; *Environ. Sci. Pollut. Res.* **2022**, *29*, 53967. [Crossref]
4. Niu, Y. F.; Chai, R. S.; Jin, G. L.; Wang, H.; Tang, C. X.; Zhang, Y. S.; *Ann. Bot.* **2013**, *112*, 391. [Crossref]
5. Lynch, J. P.; *Adv. Plant Physiol.* **2011**, *156*, 1041. [Crossref]
6. Wellmer, F. W.; Scholz, R. W.; *J. Ind. Ecol.* **2015**, *19*, 3. [Crossref]
7. Das, J.; Patra, B. S.; Baliarsingh, N.; Parida, K. M.; *Appl. Clay Sci.* **2006**, *32*, 252. [Crossref]
8. Rostami, M.; Monaco, S.; Sacco, D.; Grignani, C.; Dinuccio, E.; *Int. J. Recycling Org. Waste Agric.* **2015**, *4*, 127. [Crossref]
9. de Arruda, M. C.; Fischer, I. H.; Zanette, M. M.; da Silva, B. L.; Santos, C. D. J.; *Citrus Res. Technol.* **2011**, *32*, 103. [Link] accessed in June 2024
10. Li, H.; Dong, X.; da Silva, E. B.; de Oliveira, L. M.; Chen, Y.; Ma, L. Q.; *Chemosphere* **2017**, *178*, 466. [Crossref]
11. Liu, X.; Zong, E.; Hu, W.; Song, P.; Wang, J.; Liu, Q.; Fu, S.; *ACS Sustainable Chem. Eng.* **2018**, *7*, 758. [Crossref]
12. Kumar, P. S.; Korving, L.; Van Loosdrecht, M. C.; Witkamp, G. J.; *Water Res.: X* **2019**, *4*, 129. [Crossref]
13. Silva, J. M.: *Resíduo da Indústria Siderúrgica: Remoção Eficaz de Fosfato de Águas e Evidências de um Potencial Fertilizante*; PhD Thesis, Universidade Federal do Ceará, Fortaleza, Brazil, 2022. [Link] accessed in June 2024
14. Bezerra, M. M. M.: *Potencial de Adsorção de Fosfato por Solos Naturais em Reservatórios do Semiárido: Uma Abordagem em Microcosmos*; MSc Dissertation, Universidade Federal do Rio Grande do Norte, Natal, Brazil, 2021. [Link] accessed in June 2024
15. Tang, L.; Xie, X.; Li, C.; Xu, Y.; Zhu, W.; Wang, L.; *Mater.* **2022**, *15*, 7983. [Crossref]
16. Dávila, I. V. J.: *Adsorção de Fosfato com Dolomita Natural, Modificada por Tratamentos Térmico e Ultrassônico e Hidrotalcita Sintetizada*; PhD Thesis, Universidade Federal do Rio Grande do Sul, Porto Alegre, Brazil, 2022. [Link] accessed in June 2024
17. Sasabuchi, I.; Krieger, K. S.; Nunes, R. S.; Ferreira, A. C.; Xavier, G.; Urzedo, A. L.; Fadini, P. S.; *Quím. Nova* **2023**, *46*, 185. [Crossref]
18. Chitrakar, R.; Tezuka, S.; Sonoda, A.; Sakane, K.; Ooi, K.; Hirotsu, T.; *J. Colloid Interface Sci.* **2005**, *290*, 45. [Crossref]
19. Kuzawa, K.; Jung, Y. J.; Kiso, Y.; Yamada, T.; Nagai, M.; Lee, T. G.; *Chemosphere* **2006**, *62*, 45. [Crossref]
20. Costa, A. S.; Nascimento, A. L.; Botero, W. G.; Carvalho, C. M.; Tonholo, J.; Santos, J. C.; Anunciação, D. S.; *Sci. Total Environ.* **2022**, *802*, 149. [Crossref]
21. Rosa, L. M. T.; Botero, W. G.; Santos, J. C. C.; Cacuro, T. A.; Waldman, W. R.; do Carmo, J. B.; de Oliveira, L. C.; *J. Environ. Manage.* **2018**, *215*, 91. [Crossref]
22. Sobrinho, G. L.; de Oliveira, A. J.; Sobrinho, F. S. L.; da Silva, R. R.; de Oliveira, L. C.; Fernandes, A. P.; Botero, W. G.; *Environ. Challenges* **2021**, *2*, 110. [Crossref]
23. Rosa, L. M. T.; Botero, W. G.; do Carmo, J. B.; Gabriel, G. V.; Waldman, W. R.; Cavagis, A. D.; de Oliveira, L. C.; *Environ. Technol. Innovation* **2022**, *27*, 102452. [Crossref]
24. Reichle, W. T.; *Solid State Ionics* **1986**, *22*, 135. [Crossref]
25. Manyà, J. J.; *Environ. Sci. Technol.* **2012**, *46*, 7939. [Crossref]
26. APHA; *Standard Methods for the Examination of Water and Wastewater*; 20th ed.; Clesceri, L. S.; Greenberg, A. E.; Eaton, A. D., eds.; American Public Health Association: Washington, 1998.
27. Stelmachowski, P.; Maniak, G.; Kaczmarczyk, J.; Zasada, F.; Piskorz, W.; Kotarba, A.; Sojka, Z.; *Appl. Catal., B* **2014**, *146*, 105. [Crossref]

28. Li, Y.; Xie, X.; Liu, J.; Cai, M.; Rogers, J.; Shen, W.; *Chem. Eng. J.* **2008**, *136*, 398. [Crossref]
29. Li, L.; Qi, G.; Wang, B.; Yue, D.; Wang, Y.; Sato, T.; *J. Hazard. Mater.* **2018**, *343*, 19. [Crossref]
30. Fonseca, I.: *Síntese, Caracterização e Comportamento Eletroquímico de um Hidróxido Duplo Lamelar Baseado em Níquel e Alumínio como Material de Eletrodo para Sistemas de Armazenamento de Energia*; MSc Dissertation, Universidade Federal de Goiás, Goiânia, Brazil, 2022. [Link] accessed in June 2024
31. Kovanda, F.; Rojka, T.; Dobešová, J.; Machovič, V.; Bezdička, P.; Obalová, L.; Grygar, T.; *J. Solid State Chem.* **2006**, *179*, 812. [Crossref]
32. Silva Neto, L. D.; Anchieta, C. G.; Duarte, J. L.; Meili, L.; Freire, J. T.; *ACS Omega* **2021**, *6*, 21819. [Crossref]
33. Quesada, H. B.; Baptista, A. T. A.; Cusioli, L. F.; Seibert, D.; Bezerra, C. O.; Bergamasco, R.; *Chemosphere* **2019**, *222*, 766. [Crossref]
34. Laipan, M.; Yu, J.; Zhu, R.; Zhu, J.; Smith, A. T.; He, H.; Sun, L.; *Mater. Horiz.* **2020**, *7*, 715. [Crossref]
35. Elmoubarki, R.; Mahjoubi, F. Z.; Elhalil, A.; Tounsadi, H.; Abdennouri, M.; Sadiq, M. H.; Barka, N.; *J. Mater. Res. Technol.* **2017**, *6*, 271. [Crossref]
36. Yu, S.; Liu, Y.; Ai, Y.; Wang, X.; Zhang, R.; Chen, Z.; Wang, X.; *Environ. Pollut.* **2018**, *242*, 1. [Crossref]
37. Jaruwong, P.; Wibulswas, R.; *Asian J. Energy Environ.* **2003**, *4*, 41. [Link] accessed in June 2024
38. Anirudhan, T. S.; Ramachandran, M.; *Appl. Clay Sci.* **2007**, *35*, 276. [Crossref]
39. Huang, P.; Liang, Z.; Zhao, Z.; Cui, F.; *J. Cleaner Prod.* **2021**, *301*, 126976. [Crossref]
40. Borges, R. S.: *Remoção de Ácido Húmico Presente na Água por Adsorção em Argila Modificada por Surfatante Catiônico*; MSc Dissertation, Universidade Federal do Rio de Janeiro, Rio de Janeiro, Brazil, 2009. [Link] accessed in June 2024
41. Petzold, G.; Geissler, U.; Smolka, N.; Schwarz, S.; *Colloid Polym. Sci.* **2004**, *282*, 670. [Crossref]
42. Liu, A.; Gonzalez, R. D.; *J. Colloid Interface Sci.* **1999**, *218*, 225. [Crossref]
43. Keyikoglu, R.; Khataee, A.; Yoon, Y.; *Adv. Colloid Interface Sci.* **2022**, *300*, 102598. [Crossref]
44. Tamura, K.; Kawashiri, R.; Iyi, N.; Watanabe, Y.; Sakuma, H.; Kamon, M.; *ACS Appl. Mater. Interfaces* **2019**, *11*, 27954. [Crossref]
45. Khitous, M.; Salem, Z.; Halliche, D.; *Desalin. Water Treat.* **2016**, *57*, 15920. [Crossref]
46. Edañol, Y. D. G.; Poblador, J. A. O.; Talusan, T. J. E.; Payawan Junior, L. M.; *Mater. Today: Proc.* **2020**, *33*, 1809. [Crossref]
47. Gao, X.; Peng, Y.; Guo, L.; Wang, Q.; Guan, C. Y.; Yang, F.; Chen, Q.; *J. Environ. Manage.* **2020**, *271*, 111045. [Crossref]
48. Santos, G. E. D. S.; Lins, P. V. L.; Oliveira, L. M. T. M.; Silva, E. O.; Anastopoulos, I.; Erto, A.; Meili, L.; *J. Cleaner Prod.* **2021**, *284*, 124755. [Crossref]
49. Oliveira, D. A. V.; Botero, W. G.; Santos, J. C. C.; Silva, R. M.; Pitombo, L. M.; Carmo, J. B.; Oliveira, L. C.; *Water, Air, Soil Pollut.* **2017**, *228*, 1. [Crossref]
50. Zhang, S.; Wang, J.; Zhang, Y.; Ma, J.; Huang, L.; Yu, S.; Wang, X.; *Environ. Pollut.* **2021**, *291*, 118076. [Crossref]
51. Pahalagedara, M. N.; Samaraweera, M.; Dharmarathna, S.; Kuo, C. H.; Pahalagedara, L. R.; Gascón, J. A.; Suib, S. L.; *J. Phys. Chem. C* **2014**, *118*, 17801. [Crossref]
52. Darmograi, G.; Prelot, B.; Layrac, G.; Tichit, D.; Martin-Gassin, G.; Salles, F.; Zajac, J.; *J. Phys. Chem. C* **2015**, *119*, 23388. [Crossref]
53. Nifant'eva, T. I.; Burba, P.; Fedorova, O.; Shkinev, V. M.; Spivakov, B. Y.; *Talanta* **2001**, *53*, 1127. [Crossref]
54. Buffle, J.; Staub, C.; *Anal. Chem.* **1984**, *56*, 2837. [Crossref]
55. Burba, P.; Aster, B.; Nifant'eva, T.; Shkinev, V.; Spivakov, B. Y.; *Talanta* **1998**, *45*, 977. [Crossref]
56. Botero, W. G.; Oliveira, L. C.; Rocha, J. C.; Rosa, A. H.; Santos, A.; *J. Hazard. Mater.* **2010**, *177*, 307. [Crossref]
57. Costa Cunha, G.; Goveia, D.; Romão, L. P. C.; Oliveira, L. C.; *J. Environ. Manage.* **2015**, *154*, 259. [Crossref]
58. Sousa, P. R. D.: *Avaliação Ecotoxicológica de Herbicidas Empregado no Cultivo de Arroz Irrigado, Desenvolvimento e Validação de Método Analítico para Detecção e Quantificação de Bentazona em Água*; MSc Dissertation, Escola de Engenharia de Lorena da Universidade de São Paulo, Lorena, Brazil, 2016. [Link] accessed in June 2024
59. Souza, S. O.; Oliveira, L. C.; Cavagis, A. D.; Botero, W. G.; *Water, Air, Soil Pollut.* **2014**, *225*, 1. [Crossref]

Submitted: February 29, 2024

Published online: June 26, 2024